Broken Rotor Bar Detection in Induction Machines With Transient Operating Speeds

H. Douglas, *Student Member, IEEE*, P. Pillay, *Senior Member, IEEE*,, and A. K. Ziarani, *Member, IEEE*

Abstract—**Previous work on condition monitoring of induction machines has focused on steady-state speed operation. Here, a new concept is introduced based on an analysis of transient machine currents. The technique centers around the extraction and removal of the fundamental component of the current and analyzing the residual current using wavelets. Test results of induction machines operating both as a motor and a generator shows the ability of the algorithm to detect broken rotor bars.**

Index Terms—**Broken rotor bars, condition monitoring, wavelets.**

I. INTRODUCTION

THE most widely used methods of induction machine condition monitoring utilize the steady-state spectral components of the stator. These spectral components include voltage, current, and power and are used to detect broken rotor bars, bearing failures, and air gap eccentricity. The accuracy of these techniques depends on the loading of the machine, the signal-to-noise ratio (SNR) of the spectral components being examined, and the ability to maintain a constant speed so as to allow for the operation of the algorithm.

Broken rotor bars can be detected by monitoring the stator current spectral components [1]–[4], as identified by (1)

$$f_{sb} = f_s(1 \pm 2s) \tag{1}$$

where f_{sb} are the frequencies of sidebands due to broken rotor bars, f_s is the stator fundamental frequency, and s is the per-unit slip.

The presence of broken rotor bars is indicated by an amplitude difference of less than 50 dB between the fundamental frequency and the left sideband as shown in Figs. 1 and 2.

This method of broken rotor bar detection is based on the following assumptions.

- The speed of the machine is constant and known.
- The stator fundamental frequency is constant.
- The load is constant.
- The machine is sufficiently loaded in order to separate the sidebands from the fundamental.
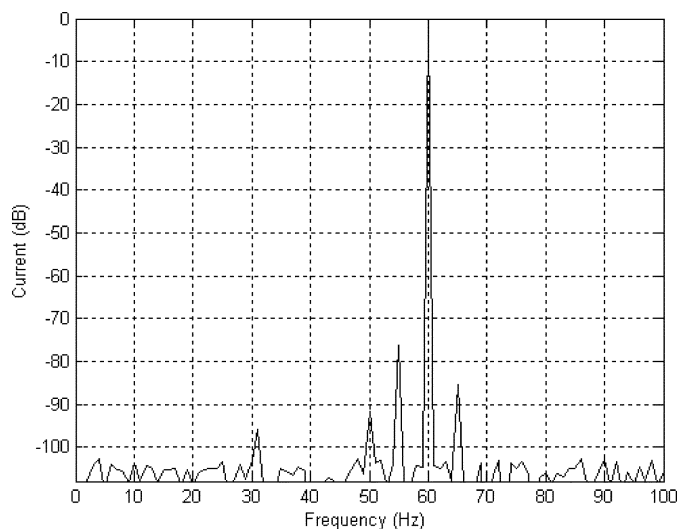
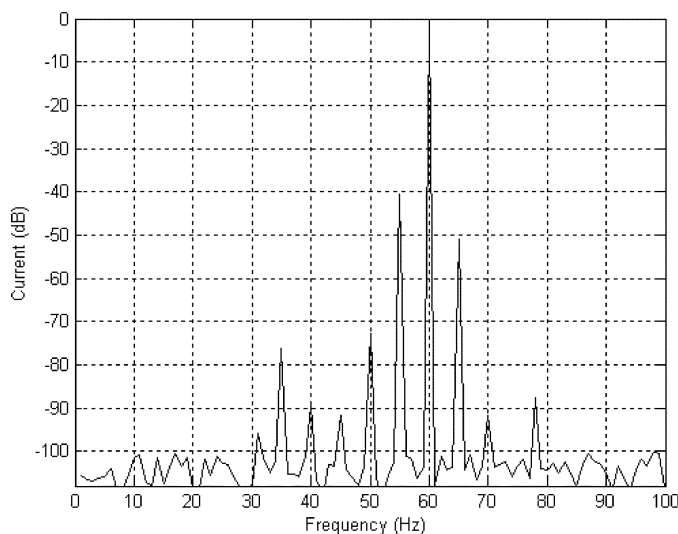Fig. 1. Typical current spectrum of a healthy induction motor.

Fig. 2. Typical current spectrum of an induction motor with broken rotor bars.

Using these assumptions and the Fourier transform, a frequency spectrum of the stator current is examined. The sideband frequencies are identified since the slip is known and assumed to be constant. The amplitude of the fundamental is then compared to that of the identified sidebands [5]–[9].

The Fourier transform shows an averaged frequency distribution, averaged amplitude and there is no time representation. Fluctuations in the instantaneous frequency and amplitude as a result of machine operation or loading effects are averaged out. It has been shown in [10] that loading conditions, which

cause these fluctuations, can produce the same frequencies associated with broken rotor bars and, therefore, make detection ambiguous. Accurate detection under transient conditions therefore cannot be easily accomplished using the Fourier transform. A detection method that utilizes time information is needed to discriminate between rotor bar frequencies and loading effects.

A disadvantage of the assumption of steady-state speed in condition monitoring is that there are many applications where constant speed is not achieved (e.g., in wind generation or motor operated valves). In addition, the steady-state algorithms focus only on low slips while improved detection can be made at high slips.

A challenge of transient analysis is the difficulty in trying to analyze the complex current transients. It consists of a nonstationary fundamental frequency as well as nonstationary frequencies associated with the rotor bars. The rotor bar frequencies change with the machine slip as do the phase and amplitude of the fundamental component. A notch filter cannot be used to separate these frequencies since it introduces a phase shift during the transient state. A filter that actively tracks the changing amplitude, phase, and frequency is needed to extract the fundamental from the transient [11]. Once the fundamental frequency has been removed, the residual transient current can be examined using wavelets [12], [13].

II. EXTRACTION OF THE NONSTATIONARY FUNDAMENTAL COMPONENT

Information about the broken rotor bars is embedded within the transient current signal. This information is largely overshadowed by the presence of the strong fundamental component which is a nonstationary sinusoidal signal due to the parameter changes during the transient. In order to enhance the efficiency of the wavelet analysis of the information-carrying signal, elimination of the fundamental component prior to wavelet analysis is proposed.

This task essentially entails extraction and subsequent subtraction of a nonstationary sinusoid from a given input signal. This section presents the adaptive algorithm employed for this task and some of its properties.

Consider a signal consisting of a sinusoid and additional signals of unknown frequency composition and expressed by

$$u(t) = A \sin(\omega t + \delta) + n(t)$$

where $n(t)$ represents the totality of the additional signal, A and ω are potentially time-varying amplitude and frequency of the sine wave, respectively, and δ is the constant phase of the sinusoid. The total phase of the sine wave is $\phi = \omega t + \delta$. If time-variations are sufficiently slow, parameters A, ω, and ϕ are constant values A_0, ω_0, and ϕ_0 within any short-time interval; otherwise, they are functions of time.

Least squares errors between the input signal $u(t)$ and the sinusoidal signal $A \sin(\omega t + \delta)$ embedded in $u(t)$ may be minimized using the gradient descent method. The result is the following set of nonlinear differential equations to govern the dynamics of a signal processing algorithm aimed at extracting the potentially nonstationary sinusoidal signal embedded in $u(t)$
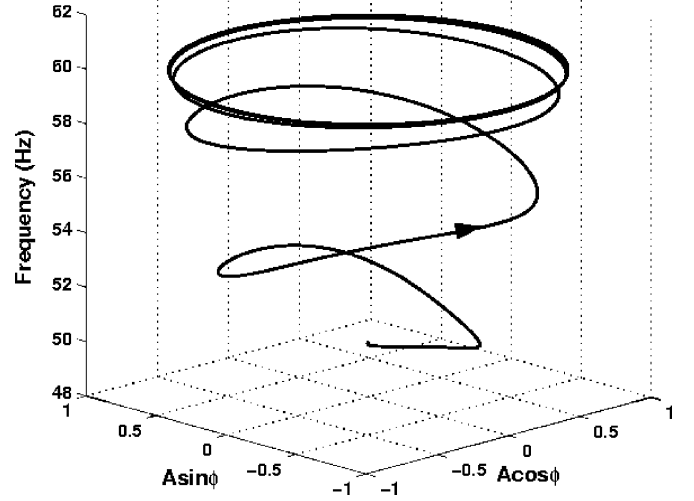

Fig. 3. Convergence to the periodic orbit ($A = 1, \omega = 120\pi, \phi = 120\pi t + \delta_0$).

without any assumption on the composition of the additional signal

$$\dot{A} = \mu_1 e \sin \phi \qquad (2)$$
$$\dot{\omega} = \mu_2 eA \cos \phi \qquad (3)$$
$$\dot{\phi} = \omega + \mu_3 \dot{\omega}. \qquad (4)$$

The dot on top () represents the differentiation with respect to time. The error signal $e(t)$ represents the difference between the input signal and the extracted sinusoid, that is

$$e(t) = u(t) - A \sin \phi. \qquad (5)$$

In the context of the present work, the error signal $e(t)$ is the information-carrying signal which will be analyzed by the wavelet transform to yield information about broken bars. Parameters μ_1, μ_2, and μ_3 are positive numbers which determine the speed of the algorithm in the estimation process as well as in tracking variations in the characteristics of the input signal over time. A more detailed presentation of the algorithm may be found in [13] where it has been shown that the algorithm exhibits adaptive nature. The mathematical proofs of the stability and convergence of the dynamical system (2)–(5) are presented in [14]. Matlab Simulink™ computational software is employed to present the performance of the algorithm. A pure sinusoid with unit amplitude, of frequency $f = \omega/2\pi = 60$ Hz, and random constant phase is input to the algorithm. The initial conditions are chosen as $A_o = 0$, $f_o = 50$, and $\phi_o = 0$. Fig. 3 shows the performance of the algorithm in convergence to the periodic orbit ($A = 1, \omega = 120\pi, \phi = 120\pi t + \delta_0$) associated with the input sinusoid.

For easy visualization, the flow of the dynamics is presented in a Cartesian coordinate system in which the axes are $A \cos \phi$, $A \sin \phi$, f. The periodic orbit, therefore, is depicted by a circle which is set off the horizontal plane at a vertical distance equal to the value of frequency. It is clear that the algorithm converges in a few cycles to the periodic orbit associated with the input sinusoid.
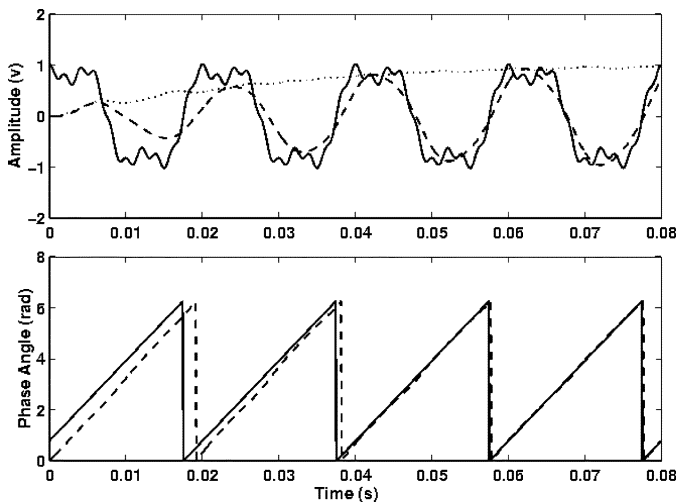
Fig. 4. Illustration of the performance of the algorithm in the extraction of the amplitude and phase of the fundamental component of a distorted sinusoid. Top: input signal (solid), extracted fundamental (dashed), and its amplitude (dotted). Bottom: actual (solid) and extracted (dashed) phase angles.
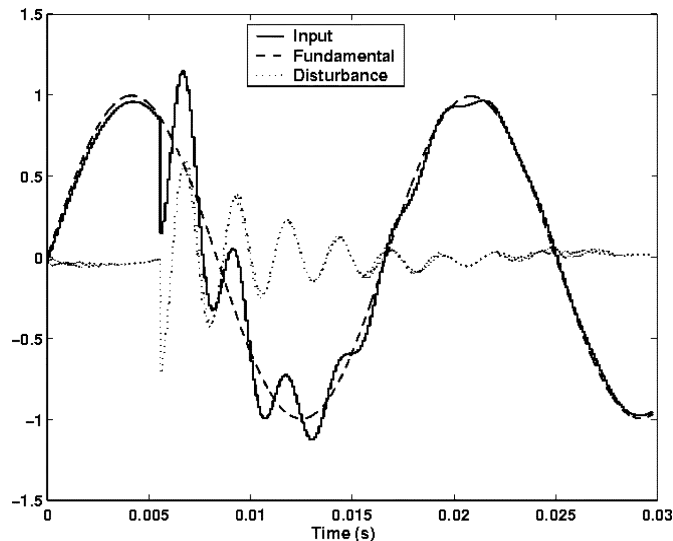

Fig. 5. Illustration of the performance of the algorithm in the detection of a disturbance imposed on a sinusoidal signal.

The values of the parameters are chosen as $\mu_1 = 100; \mu_2 = 10\,000; \mu_3 = 0.02.$ Fig. 4 shows the performance of the algorithm in the estimation of the amplitude and phase of the fundamental component of a distorted sinusoid. The values of the parameters remain the same as before in this simulation. The distortion in this case is of a harmonic form with 30% of the third and 10% of the tenth harmonic. It is observed that the amplitude and phase of the fundamental component are estimated almost within two cycles. Unlike the discrete Fourier transform-based algorithms in which only estimates of the amplitude and constant phase are computed, the fundamental component itself and, therefore, the totality of the superimposed components (i.e., $e(t)$), are instantly generated and are available in real time. This is due to the fact that the algorithm generates the total phase ϕ rather than δ.

The algorithm seeks the fundamental component of the input signal. After a transient period of a few cycles, any variation is detected in virtually no time. Fig. 5 shows the performance of the algorithm in the detection of a disturbance. As observed,
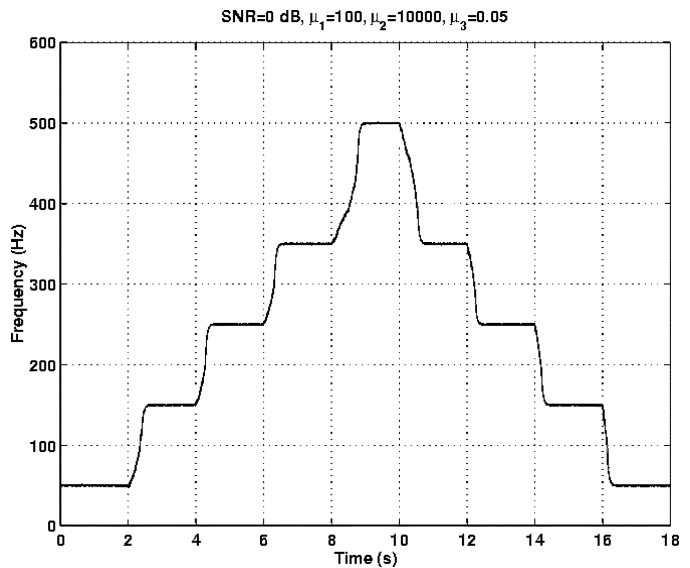

Fig. 6. Illustration of the performance of the algorithm in tracking multiple frequency jumps in noise (SNR $= 0$ dB).

once the algorithm extracts the fundamental component (dashed line), the superimposed component (dotted line) is instantly detected. This example shows the capability of the algorithm in separating the fundamental from other components present in the input signal. The algorithm is fully adaptive in tracking time-variations in the characteristics of the input signal such as the amplitude, phase, and frequency of the fundamental component. Most important, the algorithm exhibits very good performance in tracking frequency variations over time. Fig. 6 shows the performance of the algorithm in estimating multiple frequency jumps when the input signal contains a sinusoid with unit amplitude and a strong white Gaussian noise resulting in an SNR of about 0 dB.

Jumps of frequency are $50 \rightarrow 150$, $150 \rightarrow 250$, $250 \rightarrow 350$, $350 \rightarrow 500$, and back. They consecutively occur at 2-s time periods. A transient time of no more than 1 s is observed for the system to catch up with these jumps in the presence of such a strong noise. The steady-state error is observed to be independent of the value of the frequency. Parameters of the system are set as $\mu_1 = 100$, $\mu_2 = 10\,000$, and $\mu_3 = 0.05$ for this simulation.

III. Experimental Results

The experiments were conducted using an induction machine with direct online starting as well as in generator mode. Two identical rotors, with uniform rotor bar distribution, were used in this experiment except that one had a fully broken rotor bar. The same bearings and stator were used in order to minimize their influences on the transient currents. The machine was tested under loading conditions varying from 30% to 100% to determine if this method of detection could be successful and independent of the loading conditions. It was found that the motor had a very low inertia and detection could not be done below 30% loading because the transient runup times were too short.

Before implementing the fundamental extraction algorithm, the individual line currents are transformed into a single rotating
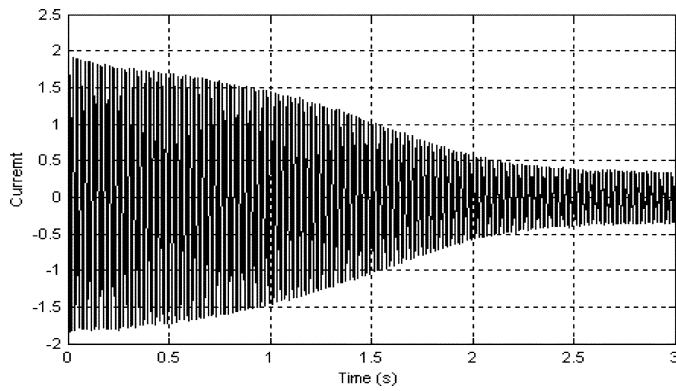
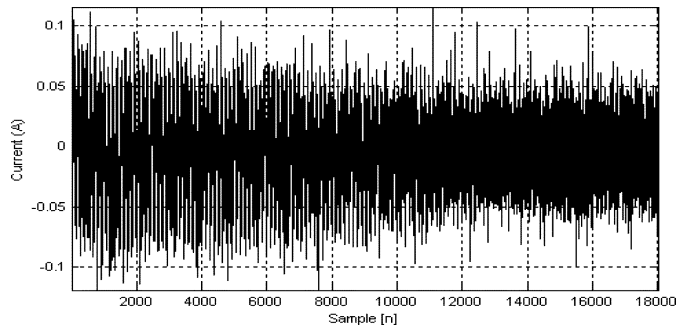Fig. 7.   Time-domain representation of the direct online staring current vector.

Fig. 8.   Startup current after extraction of the fundamental.

Fig. 9.   Wavelet decomposition levels d7-d10 of a fully loaded healthy machine.

current vector. This vector was then transformed into the time domain as shown in Fig. 7 and used as an input to the extraction algorithm. The algorithm extracts the instantaneous frequency, amplitude, and phase of the nonstationary fundamental. The resulting waveform, shown in Fig. 8, has information relating to the health of the machine including bad bearings, broken rotor bars, etc.

The extraction algorithm takes a few cycles to converge onto the amplitude and frequency of the fundamental. As a result when the estimated fundamental is subtracted from the original waveform, the algorithm's output between 0 and 0.2 s should be discarded to allow for algorithm convergence. The resulting truncated waveform is shown in Fig. 8.

The residual current is then decomposed using the discrete wavelet transform and Daubechies 8 wavelet. By examining the first six detail scales of the discrete wavelet transform, it was found that no distinction could be made between a healthy condition and the machine with the broken rotor bar. When examining scales 7–10, it is evident that there are differences in the wavelet coefficients as show in Figs. 9–12.

Figs. 9–12 show the differences and similarities between the decompositions of a 100% and 30% loaded motor. Two major features are observed by examining the detail level, d9, of the decompositions. The first feature found between samples 8–13 is found in both healthy and damaged conditions. The second feature found between samples 45–55 is only present in the decompositions of the damaged machine.

To investigate the effect of loading on the detection algorithm, the machine was loaded from 30% to 100% using direct online starting, and the level d9 of the decompositions were compared as shown in Figs. 13 and 14. It is evident that the same feature
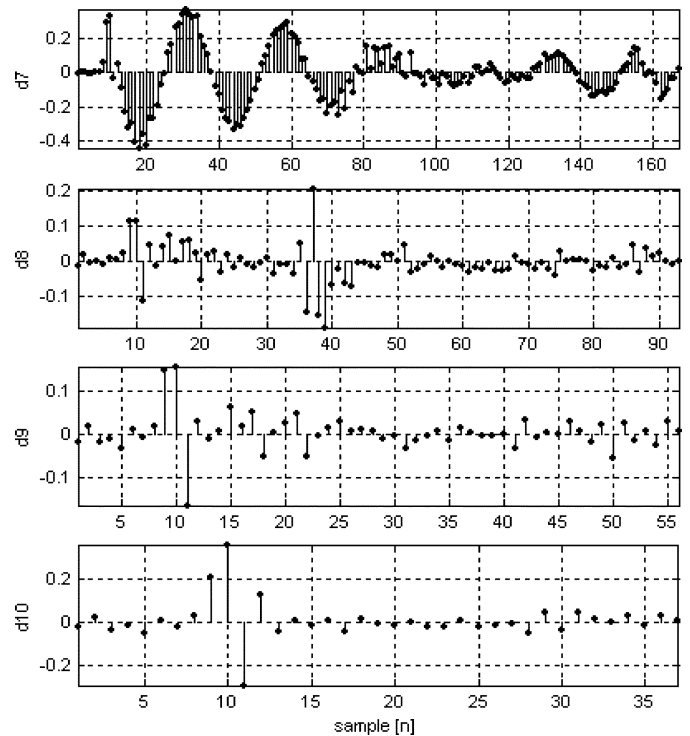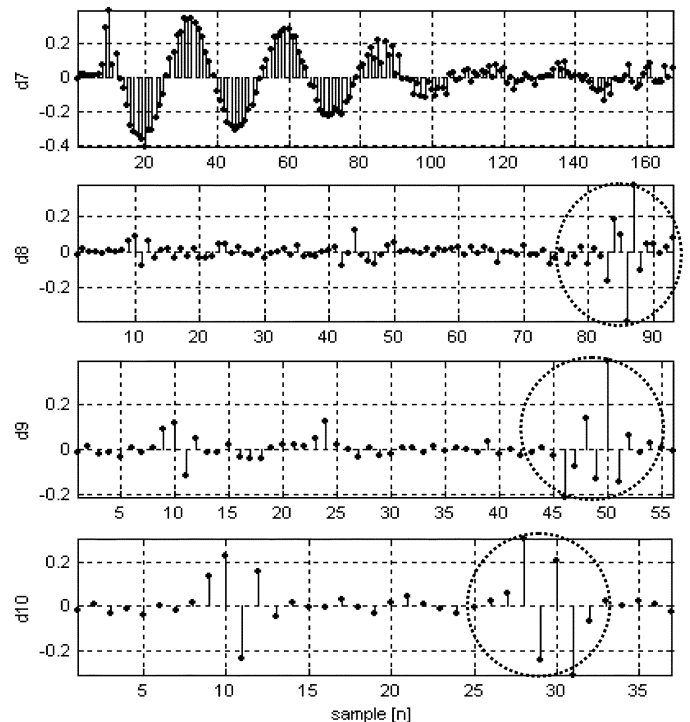

Fig. 10.   Wavelet decomposition levels d7-d10 of a fully loaded damaged machine.

difference appears throughout the loading conditions. The maximum scale needed is d9 and these results are repeatable.

The same detection methodology was applied to the machine operated as a generator. In this experiment, the generator was initially loaded to 30%. The load was increased to 100% within 3 s and the increasing transient current was captured. The extraction algorithm was used to remove the fundamental
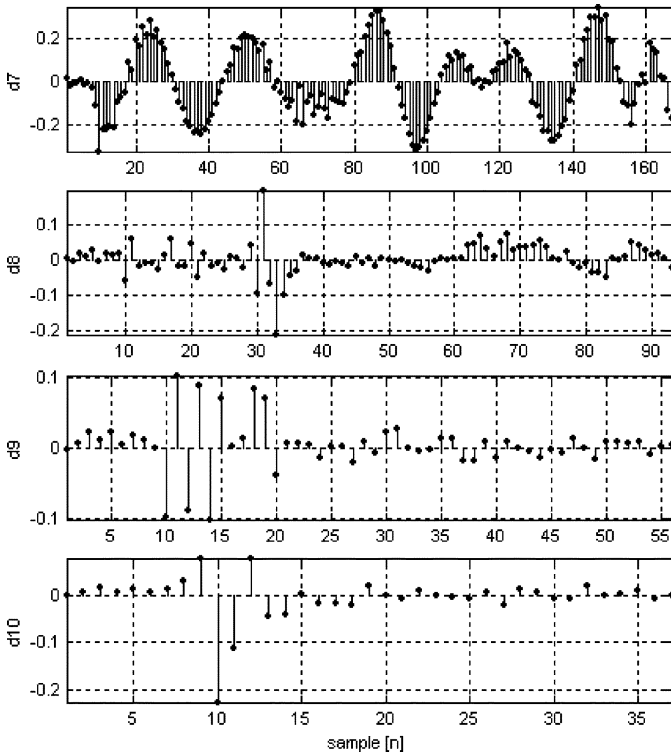
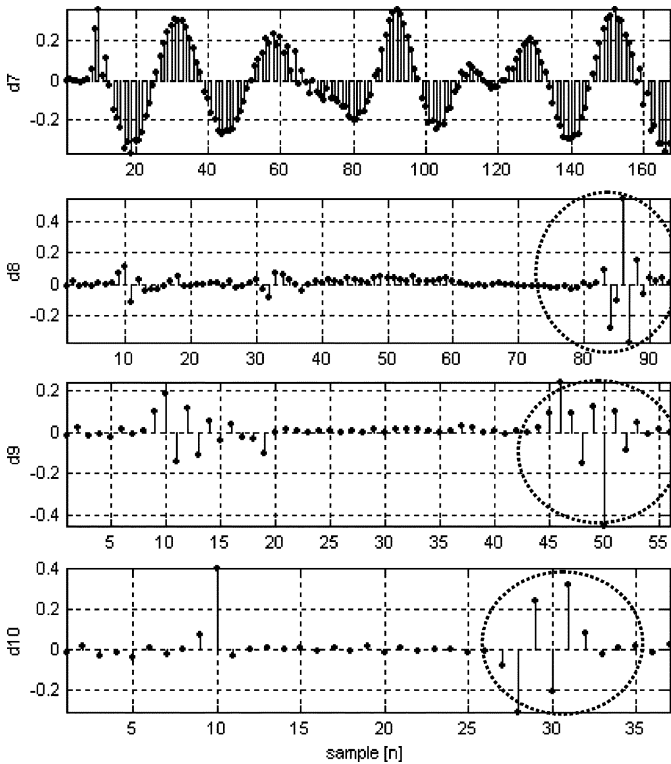Fig. 11. Wavelet decomposition levels d7-d10 of a 30% loaded healthy machine.

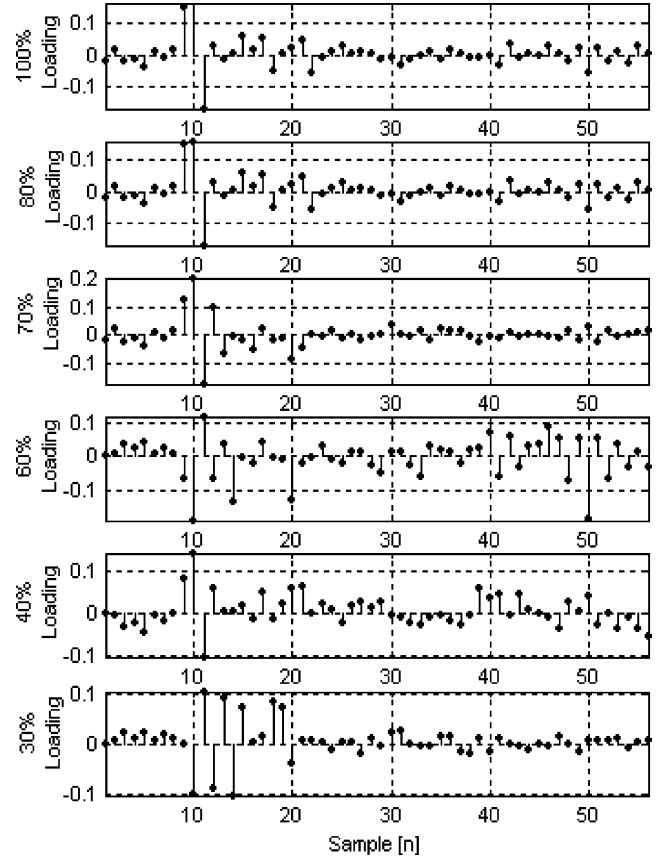Fig. 12. Wavelet decomposition levels d7-d10 of a 30% loaded damaged machine.

Fig. 13. Wavelet decomposition levels d9 of a healthy machine loaded 30% to 100%.
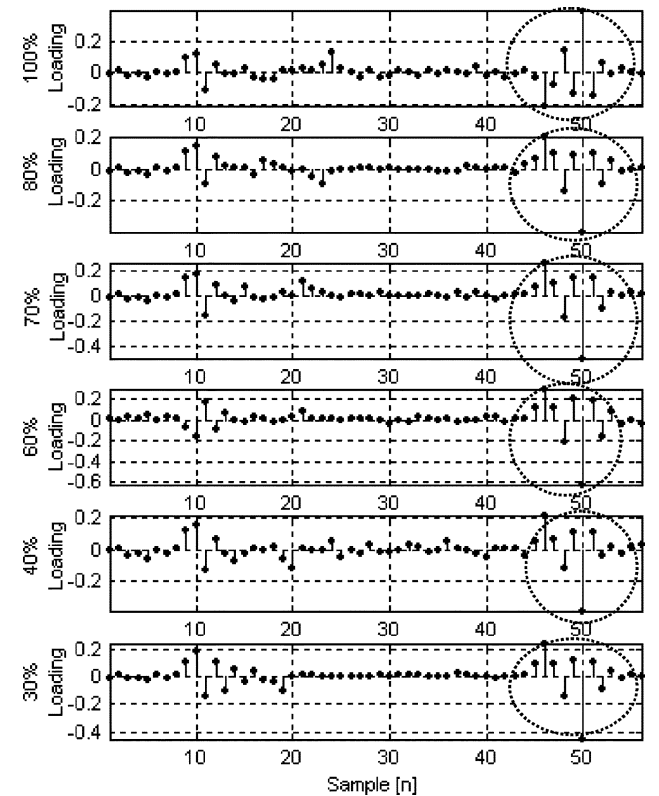
Fig. 14. Wavelet decomposition levels d9 of a damaged machine loaded 30% to 100%.

frequency and the residual current was decomposed using wavelets as shown in Figs. 15–18. The slip has not been measured in these experiments because it is not needed.

Major differences in the decompositions are observed in levels d8-d10 as shown in Fig. 19. In the case of the healthy
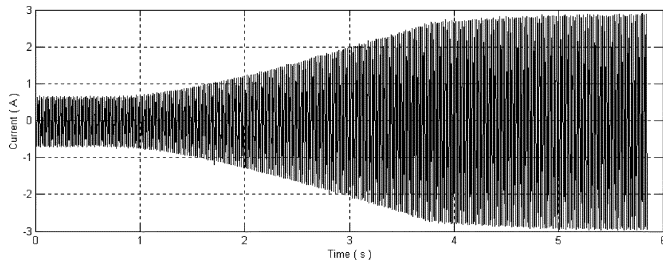
Fig. 15.   Generator phase current for a no-load to full-load change.
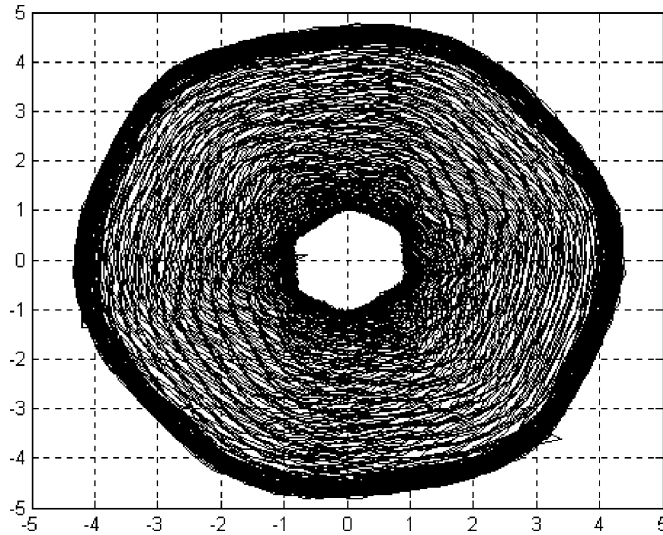

Fig. 16.   Current vector comprising all three-phase currents.
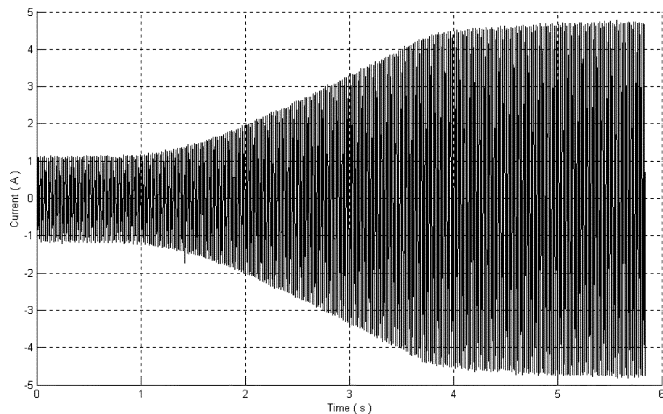

Fig. 17.   Time-domain representation of the current vector.

machine, a dominant feature is observed at samples 36–40 for level d8, 22–27 for level d9, and 15–20 of level d10.

The decomposition of the machine with the broken rotor bar is shown in Fig. 20. The dominant features are found at samples 9–12 for levels d8-d10. When observing levels 9 and 10 for both conditions, it is evident that the features in the case of the healthy machine are found in both conditions. The features indicated in Fig. 20 are only found in the case of the machine with broken rotor bar. The presence of these features can be used to formulate diagnostic algorithms to detect the presence of broken rotor bars under transient conditions.
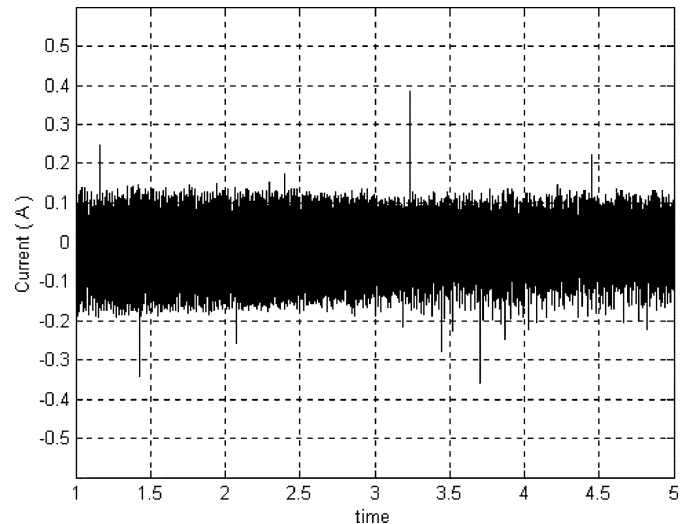

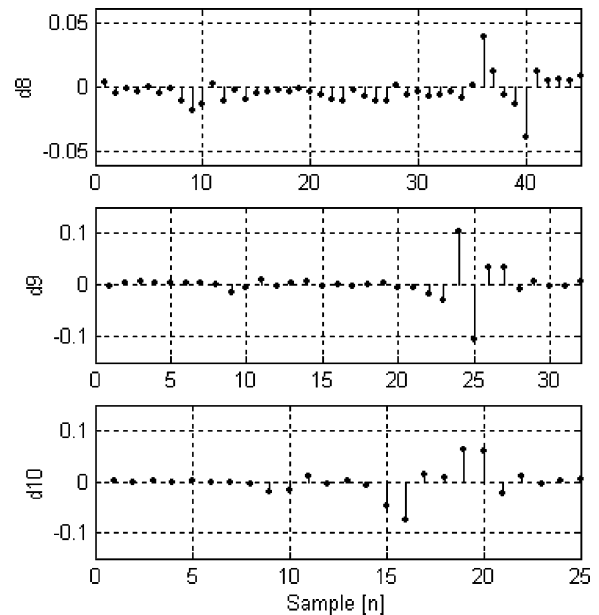Fig. 18.   Transient current after extraction of the fundamental.

Fig. 19.   Wavelet decomposition levels d8-d10 of a healthy generator.

IV. CONCLUSION

It has been shown that broken rotor bars can be detected by the decomposition of the startup current transient in motors as well as the transient current in wind generators. Constant speed is a not valid wind generator. Consequently, the steady-state algorithms previously developed are inadequate and the new algorithm should be used. This method has advantages over the traditional steady-state condition monitoring methods. It is not load dependent and can be effective on small lightly loaded machines. The machine does not have to be heavily loaded to make an accurate assessment of the machine's condition. There is no need for speed, torque, or vibration measurement.

There is the possibility that this method will be able to detect other faults such as end-ring faults, bearing failures, etc. These scenarios have not yet been investigated. However, we can assume that these faults will be detected since they will affect the current spectrum in a manner different to broken rotor bars, and other wavelet coefficients will be observed. The challenge is
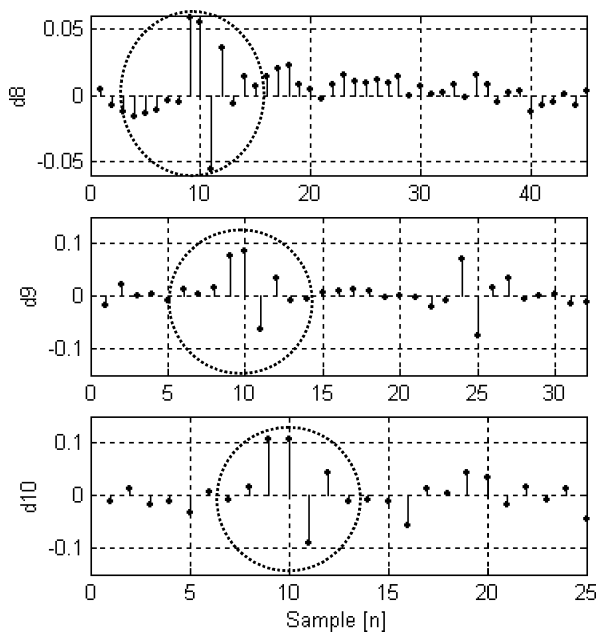
Fig. 20. Wavelet decomposition levels d8-d10 of a generator with a broken rotor bar.

being able to distinguish which wavelet coefficients represent a particular faulted condition.

The contribution here is the ability to detect a broken rotor bar while the machine is operating in the transient. It is not aimed at the detection of a specific bar at this stage. Currently, previous knowledge of a healthy machine is needed to make a diagnosis.

Different starting methods such as Y or Delta starting should not affect the detection of broken rotor bars. These starting transients will only differ in the time duration of the starting envelope. It has been shown in the results that this method is not load dependent and, therefore, should be immune to different starting methods.

Although results presented here are unique to the machine being diagnosed, the methodology applied to extracting transient fundamental currents and analysis of the residual currents can be applied generally. This method can be used for standard induction motors as well as machines that operate predominantly in the transient (e.g., wind generators or motor-operated valves).

REFERENCES

[1] M. El Hachemi Benbouzid, "A review of induction motors signature analysis as a medium for faults detection," *IEEE Trans. Ind. Electron.*, vol. 47, no. 5, pp. 984–993, Oct. 2000.
[2] R. Maier, "Protection of squirrel-cage induction motor utilizing instantaneous power and phase information," *IEEE Trans. Ind. Appl.*, vol. 28, no. 2, pp. 376–380, Mar./Apr. 1992.
[3] S. F. Legowski *et al.*, "Instantaneous power as a medium for the signature analysis of induction motors," *IEEE Trans. Ind. Appl.*, vol. 32, no. 4, pp. 904–909, Jul./Aug. 1996.
[4] A. M. Trzynadlowski *et al.*, "Diagnostics of mechanical abnormalities in induction motors using instantaneous electric power," in *Proc. IEEE Int. Electric Machines Drives Conf.*, Milwaukee, WI, 1997, pp. MB1-9.1–MB1-9.3.
[5] M. E. H. Benbouzid *et al.*, "Induction motor faults detection using advanced spectral analysis technique," in *Proc. Int. Conf. Electrical Machines*, vol. 3, Istanbul, Turkey, 1998, pp. 1849–1854.
[6] T. W. S. Chow *et al.*, "Three phase induction machines asymmetrical faults identification using bispectrum," *IEEE Trans. Energ Convers.*, vol. 10, no. 4, pp. 688–693, Dec. 1995.
[7] A. Da Silva *et al.*, "Rotating machinery monitoring and diagnosis using short-time Fourier transform and wavelet techniques," in *Proc. Int. Conf. Maintenance Reliability*, vol. 1, Knoxville, TN, 1997, pp. 14.01–14.15.
[8] G. B. Kliman *et al.*, "Methods of motor current signature analysis," *Elect. Mach. Power Syst.*, vol. 20, no. 5, pp. 463–474, Sep. 1992.
[9] W. Deleroi, "Broken bars in squirrel cage rotor of an induction motor – Part 1: Description by superimposed fault currents," *Arch. Elektrotech.*, vol. 67, pp. 91–99, 1984.
[10] W. Thompson and M. Fenger, "Case histories of current signature analysis to detect faults in induction motor drives," in *Proc. IEEE Int. Elect. Mach. Drives Conf.*, 2003, p. 1459.
[11] A. K. Ziariani and A. Konrad, "A method of extraction of sinusoids of time-varying characteristics," *Trans. Inst. Elect. Eng. Circuits Systems II: Analog Digital Signal Processing*, submitted for publication.
[12] O. Rioul and M. Vettrli, "Wavelet and signal processing," *IEEE Signal Process. Mag.*, vol. 8, no. 4, pp. 14–38, Oct. 1991.
[13] S. G. Mallat, *A Wavelet Tour of Signal Processing*. New York: Academic, 1998.
[14] A.K. Ziarani and A. Konrad, "A nonlinear adaptive method of elimination of power line interference in ECG signals," *IEEE Trans. Biomed. Eng.*, vol. 49, no. 6, pp. 540–547, Jun. 2002.
[15] M. Karimi-Ghartemani and A. K. Ziarani, "Periodic orbit analysis of two dynamical systems for electrical engineering applications," *J. Eng. Math.*, vol. 45, no. 2, pp. 135–154, 2003.
[16] P. Pillay and Z. Xu, "Motor current signature analysis," in *Proc. IEEE Ind. Appl. Soc. Annu. Meet.*, Oct. 1996, pp. 47–48.

H. Douglas (S'03) received the Bachelor's and Master's degrees from the University of Cape Town, Rondebosch, South Africa, in 1997 and 2000, respectively. He is currently pursuing the Ph.D. degree in electrical engineering at Clarkson University, Potsdam, NY.

He is a faculty member at the University of Cape Town, where he specializes in the fields of power electronics, machines, and drives. His research interests include signal processing applied to power applications.

P. Pillay (SM'92) received the Bachelor's degree from the University of Durban-Westville, Durban, South Africa, in 1981, the Master's degree from the University of Natal, Durban, South Africa, in 1983, and the Ph.D. degree from Virginia Polytechnic Institute and State University, Blacksburg, in 1987.

Currently, he is a a Professor in the Department of Electrical and Computer Engineering, Clarkson University, Potsdam, NY, where he holds the Jean Newell Distinguished Professorship in Engineering. From 1988 to 1990, he was with the University of Newcastle-upon-Tyne, Newcastle-upon-Tyne, U.K. From 1990 to 1995, he was with the University of New Orleans. He is also an Adjunct Professor at the University of Cape Town, Cape Town, South Africa. His research and teaching interests are in modeling, design, and control of electric motors and drives for industrial and alternate energy applications.

Dr. Pillay is a member of the IEEE Power Engineering, IEEE Industry Applications (IAS), IEEE Industrial Electronics, and IEEE Power Electronics Societies. He is a member of the Electric Machines Committee and Past Chairman of the Industrial Drives Committee of the IAS and Past Chairman of the Induction Machinery Subcommittee of the IEEE Power Engineering Society. He currently chairs the Awards Committee of the IAS Industrial Power Conversion Department. He has organized and taught short courses in electric drives at IAS Annual Meetings. He is a Fellow of the Institution of Electrical Engineers, U.K., and a Chartered Electrical Engineer in the U.K. He is also a Member of the Academy of Science of South Africa. He was also a recipient of a Fulbright Scholarship.

A. K. Ziarani (S'99–M'02) received the B.Sc. degree in electrical and communication systems engineering from Tehran Polytechnic University, Tehran, Iran, in 1994, and the M.A.Sc. and Ph.D. degrees in electrical engineering from the University of Toronto, Toronto, ON, Canada, in 1999 and 2002, respectively.

Currently, he is an Assistant Professor in the Department of Electrical and Computer Engineering, Clarkson University, Potsdam, NY. He is also the Co-Founder of Signamatic Technologies, Toronto, ON, Canada. His research interests include nonlinear adaptive signal processing, biomedical engineering, embedded systems design, and the theory of differential equations.